Expanded View Figures

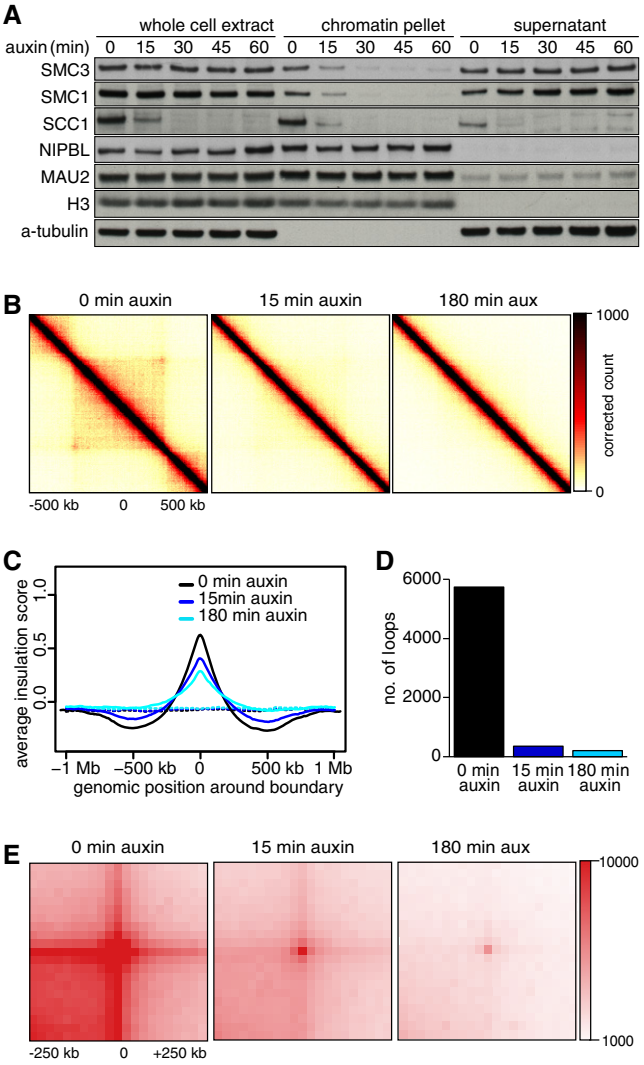

Figure EV1. Chromatin organization changes upon auxin-induced Scc1 degradation for 15 and 180 min.

A Same chromatin fractionation experiment as shown in Fig 1E. Note that the amount of cohesin loading complex, NIPBL, and MAU2, on chromatin were largely unchanged after SCC1 degradation.

B Aggregate TAD analysis for SCC1-mEGFP-AID cells expressing Tir1, at 0 (left), 15 (center), and 180 min (right) after auxin addition. Average coverage-corrected Hi-C contact matrices are shown centered around the 166 × 500–550 kb long TADs identified in the control-depleted G1 cells.

C Average insulation score around TAD boundaries identified for the control-depleted G1 cells, at 0 (black), 15 (blue), and 180 min (cyan) after auxin addition. Dashed lines show the average insulation score around the +1 Mb shifted boundaries as control.

D Number of loops identified by HiCCUPS, at 0, 15, and 180 min after auxin addition. Colors are the same as in (C).

E Total contact counts around loops after auxin addition, for all 750 kb–6 Mb long loops identified by HiCCUPS in G1 control.

Source data are available online for this figure.

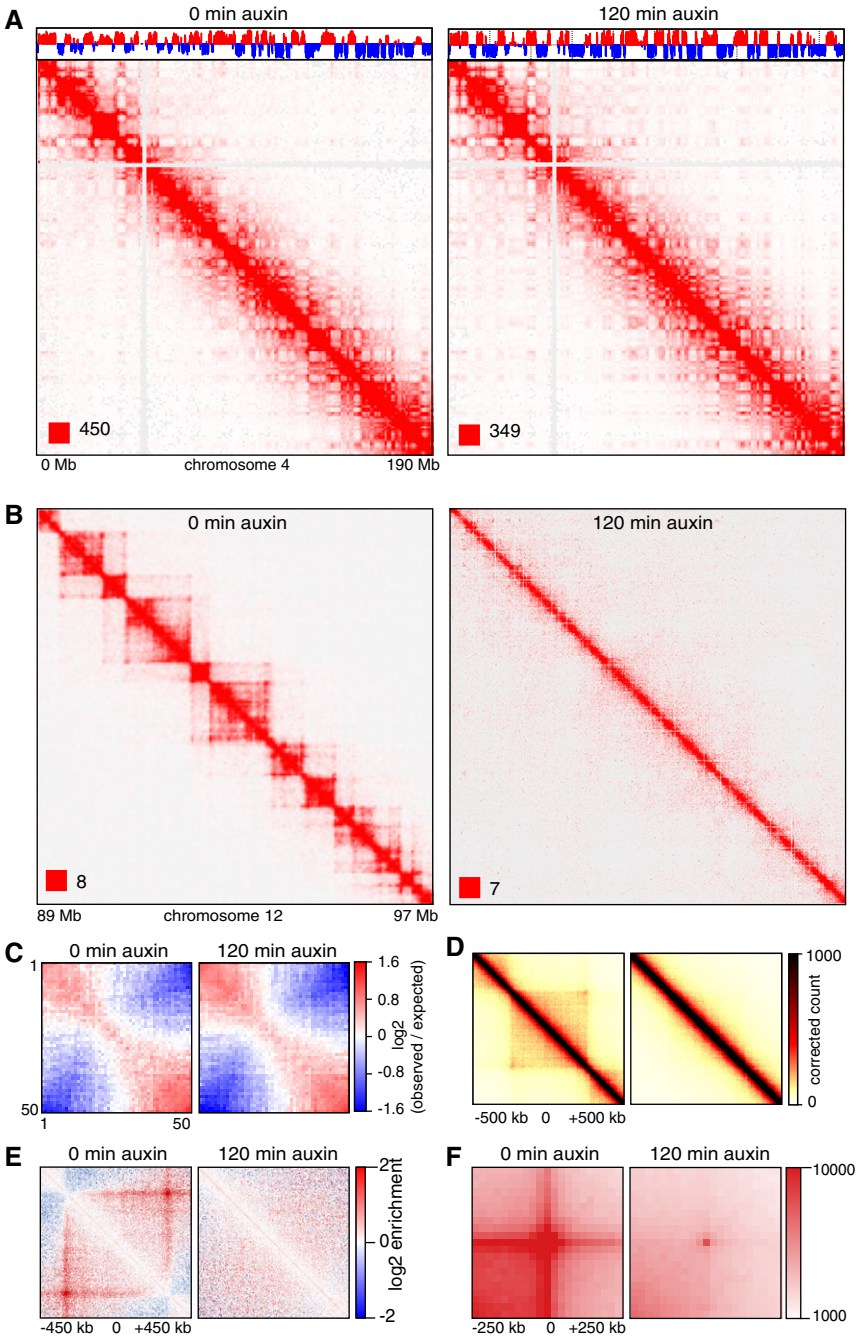

Figure EV2. Chromatin organization changes upon auxin-induced Scc1 degradation for 15 and 120 min.

A Coverage-corrected Hi-C contact matrices of chromosome 4, at 0 and 120 min after auxin addition in SCC1-mEGFP-AID cells. The corresponding compartment signal tracks at 250 kb bin resolution are shown above the matrices. The matrices were plotted using Juicebox.

B For the same conditions, coverage-corrected Hi-C contact matrices in the 89–97-Mb region of chromosome 12, plotted by using Juicebox.

C Inter-chromosomal contact enrichment between 250 kb bins with varying compartment strength from most B-like (1) to most A-like (50), in SCC1-mEGFP-AID control cells in a replicate experiment, at 0 and 120 min after auxin addition.

D Aggregate TAD analysis for CTCF-mEGFP-AID cells expressing Tir1, 0 (left) and 120 min (right) after auxin addition. Average coverage-corrected Hi-C contact matrices are shown centered around the 166 × 500–550 kb long TADs identified in the control-depleted HeLa cells.

E Average contact enrichment around loops after auxin addition in SCC1-mEGFP-AID cells, for the 82 × 600 kb long loops identified by HiCCUPS in G1 control. The matrices are centered (0) around the halfway point of the loop anchor coordinates.

F Total contact counts around loops after auxin addition in SCC1-mEGFP-AID cells, for all 750 kb–6 Mb long loops identified by HiCCUPS in G1 control.

Figure EV3. Depletion of Wapl and PDS5 proteins does not change localization and levels of condensin.

A Live-cell imaging of SCC1-mEGFP, CAP-D2-mEGFP, and CAP-D3-mEGFP cells in which all alleles of these genes were C-terminally fused to a mEGFP tag by CRISPR/Cas9 engineered genome editing. Representative cells at interphase, prophase, and prometaphase are shown. DNA was stained with SiR-DNA by Spirochrome. Scale bar indicates 5 μm.

B Live-cell imaging of SCC1-mEGFP, CAP-D2-mEGFP, and CAP-D3-mEGFP cells depleted for control or WAB by RNAi. DNA was stained with SiR-DNA by Spirochrome. Scale bar indicates 10 μm.

C Immunofluorescence images of CAP-D3-mEGFP cells depleted for SMC2, WAB, or SMC2/WAB. GFP staining was used as readout for estimating condensin depletion efficiency. Scale bar indicates 5 μm.

D Quantification of immunofluorescence intensities for GFP signal in cells depleted for control and SMC2 is shown. Error bar depicts standard deviations of the means. Data from 2 replicates.

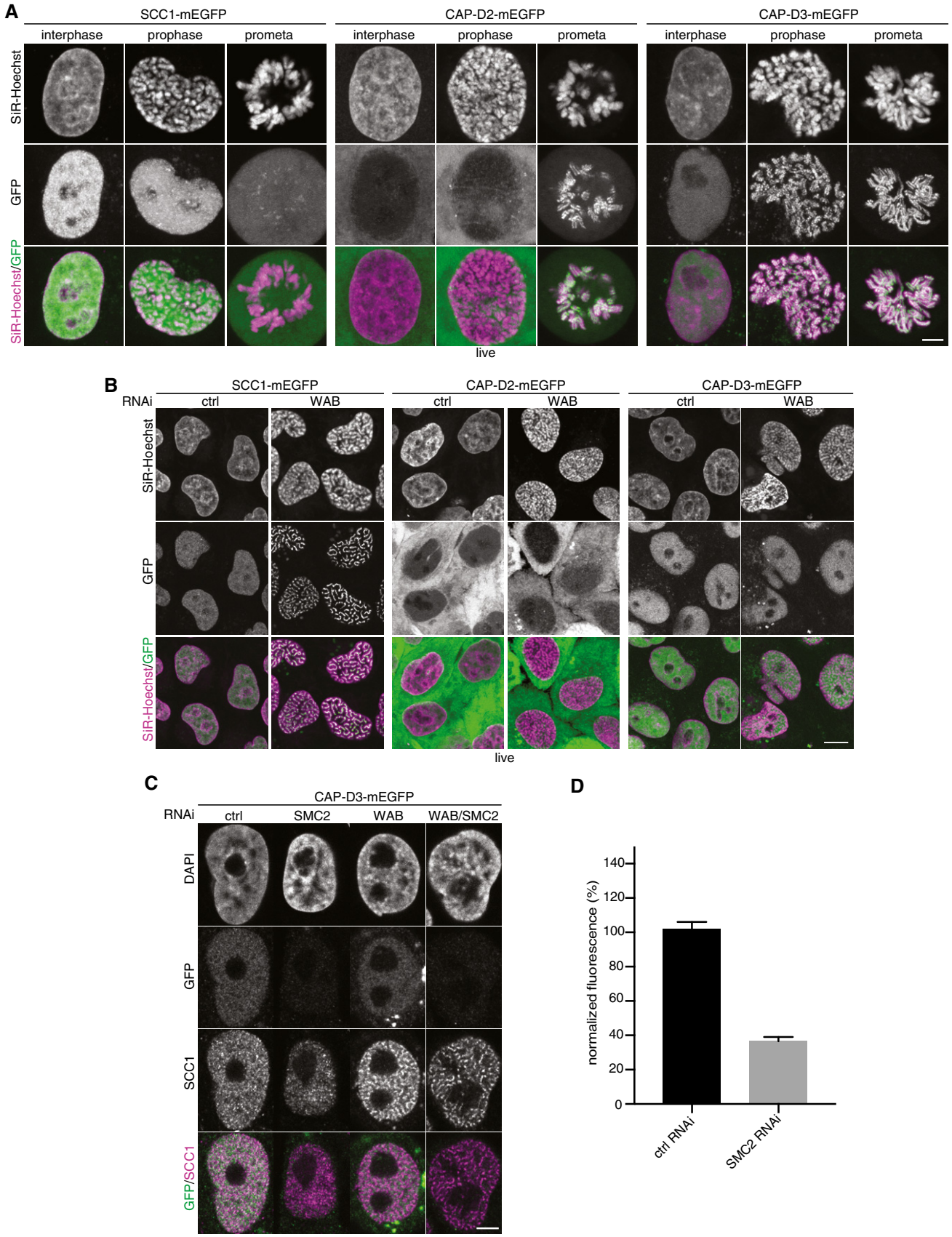

Figure EV3.

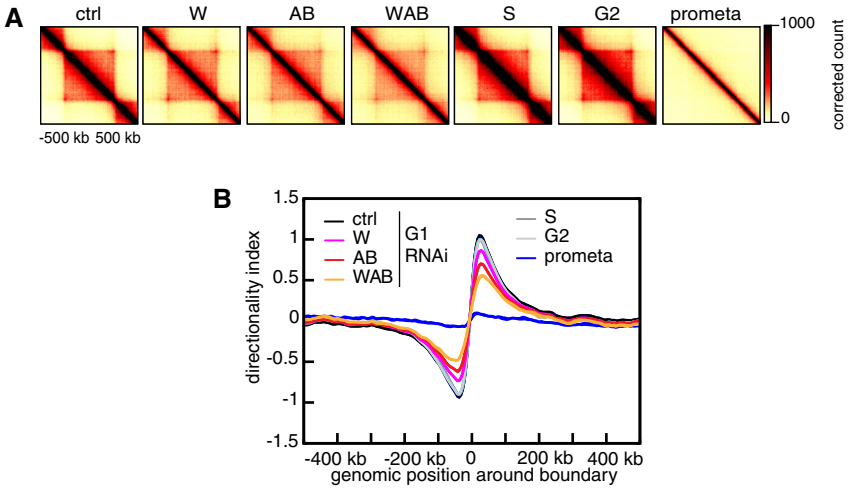

Figure EV4. Insulation decreases upon depletion of WAPL and PDS5 proteins.

A Aggregate TAD analysis for control-depleted (ctrl), WAPL-depleted (W), PDS5A/PDS5B-depleted (AB), joint WAPL/PDS5A/PDS5B-depleted (WAB) cells in G1-phase, as well as S-phase (S), G2-phase (G2), and prometaphase (prometa) cells. Average coverage-corrected Hi-C contact matrices are shown centered around the 166 × 500–550 kb long TADs identified in the control-depleted G1 cells.

B Average standardized directionality index profiles in a 1 Mb region centered around TAD boundaries identified in the control-depleted cells, for the same conditions as in (A). Colors are as in Fig 7B.

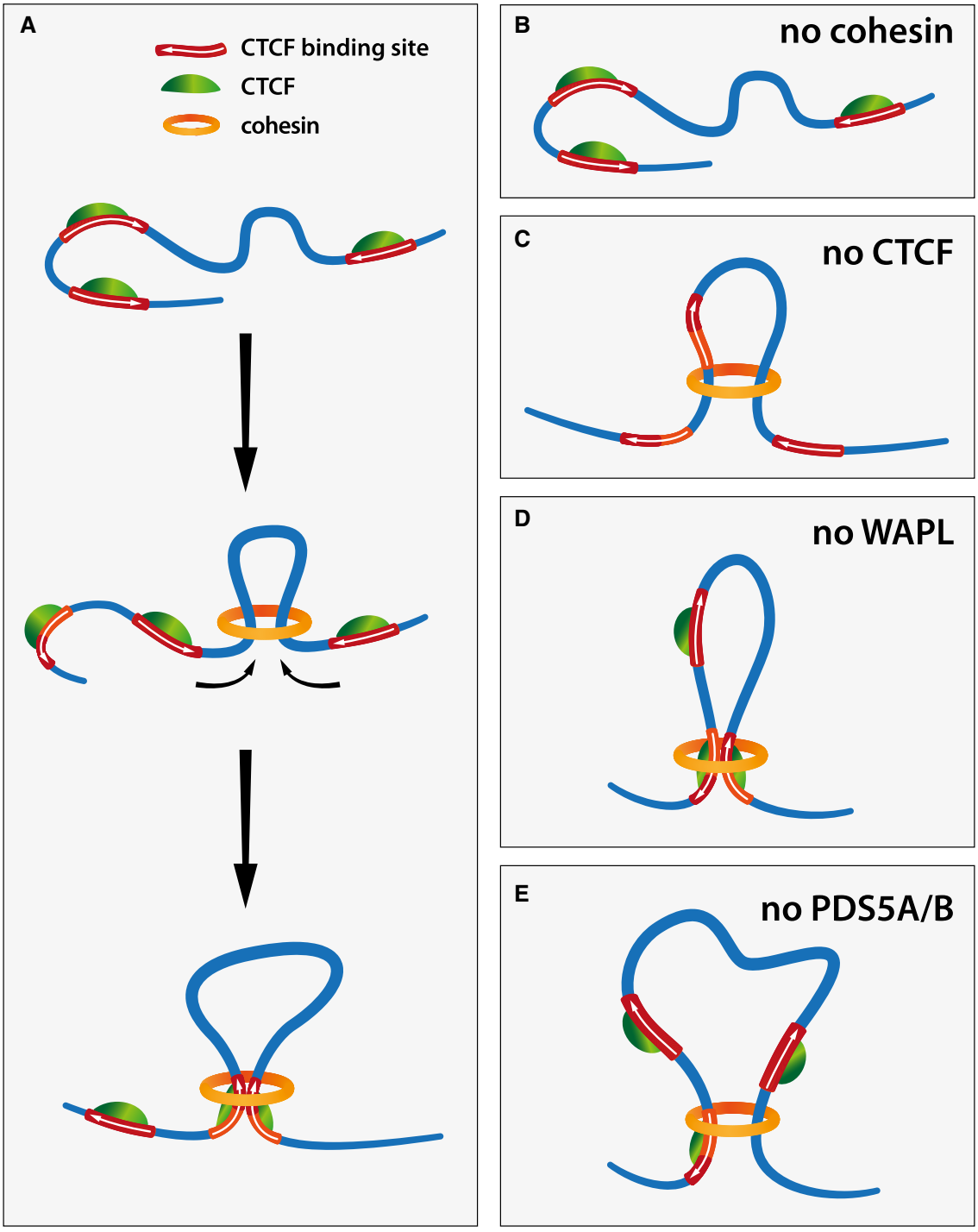

Figure EV5. Loop formation depends on cohesin and is regulated by CTCF, WAPL, and PDS5 proteins.

A Graphical illustration of how cohesin might mediate loop extrusion. Cohesin binds to chromatin, extrudes a chromatin loop and stalls upon encountering CTCF bound at convergently oriented CTCF sites.

B In the absence of cohesin, chromatin loops are eliminated.

C In the absence of CTCF, cohesin extrudes chromatin loops but fails to stall at convergently oriented CTCF binding sites.

D, E In the absence of WAPL (D) or PDS5A/B (E), cohesin extrudes longer chromatin loops, which occur more frequently between regions of non-convergent (D) or single CTCF sites (E). While in the absence of Wapl loop extrusion still halts at occupied CTCF sites, in the absence of PDS5A/B loop extrusion may halt less readily, resulting in fewer specific loops called.